Rotational spectrum and structure of the (OCS)2–C2H4 trimer: Example of a polar OCS dimer

ARTICLE *in* JOURNAL OF MOLECULAR STRUCTURE · JULY 2002

Impact Factor: 1.6 · DOI: 10.1016/S0022-2860(02)00097-2

3 AUTHORS, INCLUDING:

Rebecca A Peebles
Eastern Illinois University
61 PUBLICATIONS **315** CITATIONS
SEE PROFILE

Sean A Peebles
Eastern Illinois University
96 PUBLICATIONS **785** CITATIONS
SEE PROFILE

ELSEVIER

Journal of Molecular Structure 612 (2002) 261–275

Journal of
MOLECULAR
STRUCTURE

www.elsevier.com/locate/molstruc

Rotational spectrum and structure of the $(OCS)_2$–C_2H_4 trimer: example of a polar OCS dimer ☆

Rebecca A. Peebles, Sean A. Peebles[1], Robert L. Kuczkowski*

Department of Chemistry, University of Michigan, 930 N. University Avenue, Ann Arbor, MI 48109-1055, USA

Received 25 June 2001; revised 24 October 2001; accepted 24 October 2001

Abstract

The rotational spectra for seven isotopomers of the OCS–OCS–C_2H_4 trimer have been observed with a Fourier transform microwave spectrometer. Their moments of inertia were fitted to a structure in which the plane of the ethylene is roughly parallel to a plane formed by the OCS monomers aligned with parallel dipoles. Dipole moment measurements and semi-empirical modeling confirmed this geometry. The transitions were split into doublets separated by 30–100 kHz by a tunneling motion in the complex. Isotopic studies indicated that this motion involved rotation of the ethylene in its molecular plane. The structure of the trimer is very similar to the HCCH–$(OCS)_2$ trimer in which the dipoles of the two OCS monomers were also aligned parallel. The complex is compared with several dimers containing ethylene which also show tunneling motions.

Keywords: $(OCS)_2$–C_2H_4; Weak complex; Rotational spectrum; Intermolecular forces

1. Introduction

The structures of many weakly bound dimer species have been investigated by Fourier transform microwave (FT-MW) spectroscopy since this method was introduced by Balle and Flygare about twenty years ago [1]. Investigation of such weakly bound dimers leads to information on intermolecular forces in these species, serving as a test and guide for theoretical work. Recently, the investigation of trimers of linear monomers [2–14] has helped extend the methodology to more complex systems. The comparison of trimers and related dimers leads to insight into the small changes that usually occur when a third body is added to a dimer system. Experimentally observed changes between dimer and trimer structures can be compared with theoretical results, to determine whether a model gives a reasonable representation of the intermolecular forces that could be extended to even larger systems. This fosters a theoretical understanding of more complex systems and ultimately condensed phases.

The study of trimers that contain two linear and one non-linear molecule is a first step beyond a system of three linear monomers. One of the few examples of this type of species to be investigated by FT-MW was the trimer SO_2–$(N_2O)_2$ [15]. The current paper investigates the C_2H_4–$(OCS)_2$ system. This complex is

☆ This paper is dedicated to Professor Paolo G. Favero and Professor Helmut Dreizler in appreciation of their significant contributions to the field of microwave spectroscopy.

* Corresponding author. Tel.: +1-734-763-6148; fax: +1-734-647-4865.

E-mail address: kuczkows@umich.edu (R.L. Kuczkowski).

[1] Present address: Department of Chemistry, Eastern Illinois University, 600 Lincoln Avenue, Charleston, IL 61920, USA.

0022-2860/02/$ - see front matter
PII: S0022-2860(02)00097-2

Table 1
Transition frequencies ν (MHz) and residuals $\Delta\nu$ (kHz) for $(OCS)_2$–C_2H_4 and $(O^{13}CS)_2$–C_2H_4

$J'_{K'_aK'_c}$	$J''_{K''_aK''_c}$	$(OCS)_2$–C_2H_4		$(O^{13}CS)_2$–C_2H_4	
		ν	$\Delta\nu$	ν	$\Delta\nu$
3_{12}	2_{02}	5615.2742	2.8	5558.2777	−2.7
3_{22}	2_{11}	6007.6638	0.4	5978.5634	4.9
3_{21}	2_{11}	6163.9018	0.9	6126.5261	3.7
3_{22}	2_{12}	6479.6823	−2.9	6439.0810	0.9
3_{21}	2_{12}	6635.9223	−0.3	6587.0444	0.4
3_{31}	2_{20}	7339.6036	−0.9	7315.7757	−1.0
3_{30}	2_{20}	7344.0355	1.1	7319.8161	−0.9
3_{31}	2_{21}	7372.5618	−1.1	7346.8907	−1.9
3_{30}	2_{21}	7376.9899	−2.9	7350.9338	0.9
4_{04}	3_{13}	5616.1053	−3.4		
4_{14}	3_{13}	5735.1670	1.2	5678.7400	0.6
4_{04}	3_{03}	5836.5827	−3.5	5782.0022	0.0
4_{14}	3_{03}	5955.6466	3.3	5908.5408	−5.3
4_{23}	3_{22}	6078.6109	−2.3	6013.2268	3.2
4_{31}	3_{30}			6113.1305	0.3
4_{13}	3_{12}	6338.6967	−0.2	6269.1614	−1.6
4_{22}	3_{21}	6346.0660	−1.1	6268.4656	−0.7
4_{23}	3_{12}	7295.0489	0.1	7255.0484	−0.9
4_{13}	3_{03}	7498.7685	2.4	7415.9566	2.6
4_{22}	3_{12}	7718.7433	3.1	7658.2543	−1.5
4_{23}	3_{13}			8172.0305	−3.2
4_{32}	3_{21}	8797.0576	−0.5		
4_{31}	3_{21}	8827.2495	−6.3		
4_{41}	3_{30}	9992.3826	0.7	9961.1331	−0.7
4_{40}	3_{30}	9992.8766	3.1	9961.5672	0.1
4_{41}	3_{31}	9996.8122	0.4	9965.1743	0.2
4_{40}	3_{31}	9997.3006	−2.8	9965.6085	1.1
5_{05}	4_{14}	7073.3705	0.8	6999.5036	0.0
5_{15}	4_{14}	7130.9600	2.6	7061.9728	−1.4
5_{05}	4_{04}	7192.4255	−1.3	7126.0505	3.0
5_{15}	4_{04}	7250.0166	2.1	7188.5186	0.5
5_{24}	4_{23}	7557.5533	2.7		
5_{32}	4_{31}	7789.4110	−2.3		
5_{14}	4_{13}	7833.2692	−2.0		
5_{23}	4_{22}	7991.7559	1.1		
5_{24}	4_{13}	8513.9030	0.5		
5_{14}	4_{04}	9495.4503	−0.7		
6_{06}	5_{15}	8489.0044	1.4		
6_{16}	5_{15}	8514.8769	−0.9		
6_{06}	5_{05}	8546.5914	0.7		
6_{16}	5_{05}	8572.4625	−3.0		

particularly interesting because of the known related dimers and trimers with which it can be compared. For example, the recently studied HCCH–$(OCS)_2$ trimer [7] and OCS–C_2H_4 dimer [16] are similar structurally to the title complex. These species will be compared and the success of a semi-empirical model [17] will be discussed.

2. Experimental

The rotational spectra of the normal species and six additional isotopomers were observed with the two University of Michigan Fourier-transform microwave spectrometers [18]. These spectrometers incorporate hardware and software improvements from the University of Kiel [19], allowing scans of up to several hundred MHz with minimal intervention by the operator. For the initial scans, a gas mixture of approximately 1.5% of each component (ethylene and OCS) was diluted in first-run He/Ne (10% He, 90% Ne) to a backing pressure of 2–3 bar. Previous experience with trimeric systems has indicated that the intensity of the trimer transitions is particularly sensitive to the expansion conditions. To ensure that these conditions did not vary too dramatically during the searching, the backing pressure was not allowed to drop below 2 bar. This improved the chances of initially observing the maximum number of trimer transitions. The initial searches were carried out using a General Valve Corporation Series 9 pulsed supersonic nozzle. This nozzle was mounted perpendicular to the axis of microwave propagation. This gave transitions with a full-width at half-maximum of 30 kHz. The center frequencies were accurate to about 4 kHz. The transitions were doubled due to a tunneling motion, with splittings ranging from about 30 to 100 kHz. Average frequencies of the tunneling doublets were used for fitting and analyzing the spectra. Following the initial assignment of the spectrum, Stark effects were measured using a modified Bosch fuel injector nozzle with the second spectrometer. The position of the nozzle and the resultant lineshapes were the same. After experimenting with sample concentrations, it was determined that a mixture of about 3% OCS and 1.5% C_2H_4 gave a better signal intensity. This is in contrast to other trimers investigated by us where a 1:1 ratio of components was satisfactory. Maximum signal-to-noise (S/N) for the normal isotopomer was about six after averaging for 300 cycles.

Stark effect measurements were carried out by applying voltages of up to ± 7 kV to a pair of steel

Table 2
Transitionfrequencies ν (MHz) and residuals $\Delta\nu$ (kHz) for isotopomers of $(OCS)_2$–C_2H_4 with substitution in one monomer (the first $O^{13}CS$ species has the ^{13}C at atom 5 in Fig. 1. The second $O^{13}CS$ species has the ^{13}C at atom 2. The deuteriums in the 1,1-$C_2D_2H_2$ species are at atoms 8 and 9. The deuteriums in the *cis*-1,2-$C_2D_2H_2$ species are at atoms 8 and 11 or 9 and 12; site ambiguous)

$J'_{K'_aK'_c}$	$J''_{K''_aK''_c}$	$O^{13}CS$–$O^{12}CS$–C_2H_4		$O^{12}CS$–$O^{13}CS$–C_2H_4		$(OCS)_2$–1,1-$C_2D_2H_2$		$(OCS)_2$–$^{13}C_2H_4$		$(OCS)_2$–*cis*-1,2-$C_2D_2H_2$	
		ν	$\Delta\nu$	ν	$\Delta\nu$	ν	$\Delta\nu$	ν	$\Delta\nu$	ν	$\Delta\nu$
3_{21}	2_{11}	6145.1260	9.0	6145.2353	−10..9	5999.3704	−0.5	6020.2786	5.0	6004.2263	1.8
3_{22}	2_{12}	6458.9073	−12.0	6459.8234	3.0	6316.4364	2.4	6334.9216	1.9	6315.8305	3.5
3_{31}	2_{20}	7323.6498	−5.3	7331.7728	−5.6	7066.0798	−1.5	7098.7121	−4.5	7086.6799	−13.5
3_{30}	2_{20}	7327.9130	−1.6	7335.9760	−3.8	7072.7078	0.8	7104.8140	−1.2	7092.4132	−3.5
3_{31}	2_{21}	7355.7886	−0.3	7363.6891	−2.1	7107.8368	−6.2	7138.3665	−0.1	7124.7377	−2.8
3_{30}	2_{21}	7360.0509	2.4	7367.9020	9.4	7114.4680	−0.6	7144.4635	−1.8	7130.4706	6.8
4_{13}	3_{12}	6310.0447	6.6	6297.8283	8.8	6268.9080	2.3	6284.7790	−2.2	6261.2271	−0.1
4_{32}	3_{22}	8928.5055	−2.6	8932.9162	0.0	8683.3909	1.2	8715.2760	1.2	8693.9899	9.2
4_{41}	3_{30}	9970.8541	−3.2	9982.7217	5.5	9618.8490	−0.7	9662.2681	−0.6	9645.4582	0.0
4_{40}	3_{30}	9971.3284	4.9	9983.1785	5.6	9619.7152	−1.2	9663.0402	−2.2	9646.1678	−0.5
4_{41}	3_{31}	9975.1208	3.9	9986.9161	−1.5	9625.4766	1.2	9668.3693	1.9	9651.1860	4.5
4_{40}	3_{31}	9975.5840	0.9	9987.3695	−4.8	9626.3465	4.4	9669.1439	2.8	9651.8889	−2.8
5_{05}	4_{14}									6968.0964	−0.3
5_{15}	4_{14}	7104.1171	−14.2	7088.8893	0.7	6986.7395	0.8	7023.7849	−3.4	7009.8183	3.6
5_{05}	4_{04}	7166.5202	10.7	7152.0670	2.6	7033.8941	1.3	7073.1320	4.8	7060.5333	2.3
5_{15}	4_{04}									7102.2496	0.5
5_{14}	4_{13}	7799.9641	−0.1	7785.4071	−8.0	7718.3152	−4.6	7744.6944	−1.7	7720.1714	−9.8

Table 3
Spectroscopic constants for $(OCS)_2$–C_2H_4

	$(OCS)_2$–C_2H_4	$(O^{13}CS)_2$–C_2H_4	$O^{13}CS$–$O^{12}CS$–C_2H_4[a]	$O^{12}CS$–$O^{13}CS$–C_2H_4[b]	$(OCS)_2$– 1,1-$C_2D_2H_2$[c]	$(OCS)_2$–$^{13}C_2H_4$	$(OCS)_2$–*cis*-1,2-$C_2D_2H_2$[d]
A (MHz)	1318.1772(4)	1314.9157(4)	1315.5893(11)	1317.5120(9)	1266.0679(4)	1271.9581(7)	1269.9353(12)
B (MHz)	841.7726(4)	831.4975(7)	837.4374(16)	835.8162(14)	839.4620(6)	839.7355(11)	835.3920(20)
C (MHz)	684.4232(3)	677.9820(5)	681.9870(22)	680.4271(19)	668.9088(9)	673.0485(15)	672.0718(27)
Δ_J(kHz)	0.982(7)	0.937(15)	0.951(39)	0.983(33)	0.903(16)	0.976(27)	0.951(50)
Δ_{JK}(kHz)	0.612(34)	0.633(53)	0.61[e]	0.61[e]	0.61[e]	0.61[e]	0.61[e]
Δ_K(kHz)	1.283(28)	1.279(47)	1.28[e]	1.28[e]	1.28[e]	1.117(47)	0.892(89)
δ_J(kHz)	0.153(3)	0.129(7)	0.15[e]	0.15[e]	0.15[e]	0.15[e]	0.15[e]
δ_K(kHz)	1.299(51)	1.29(10)	1.3[e]	1.3[e]	1.3[e]	1.3[e]	1.3[e]
$\Delta\nu_{rms}$(kHz)[f]	2.01	2.13	6.73	5.78	2.59	2.75	5.37
N[g]	38	28	15	15	15	15	17

[a] C_5 substituted.
[b] C_2 substituted.
[c] d_8, d_9 substituted.
[d] Location of substitution is unclear, either at sites 8, 11 or 9, 12, see text.
[e] Fixed at value from normal $(OCS)_2$–C_2H_4.
[f] $\Delta\nu_{rms} = (\sum(\nu_{obs} - \nu_{calc})^2/N)^{1/2}$.
[g] N = number of lines in fit.

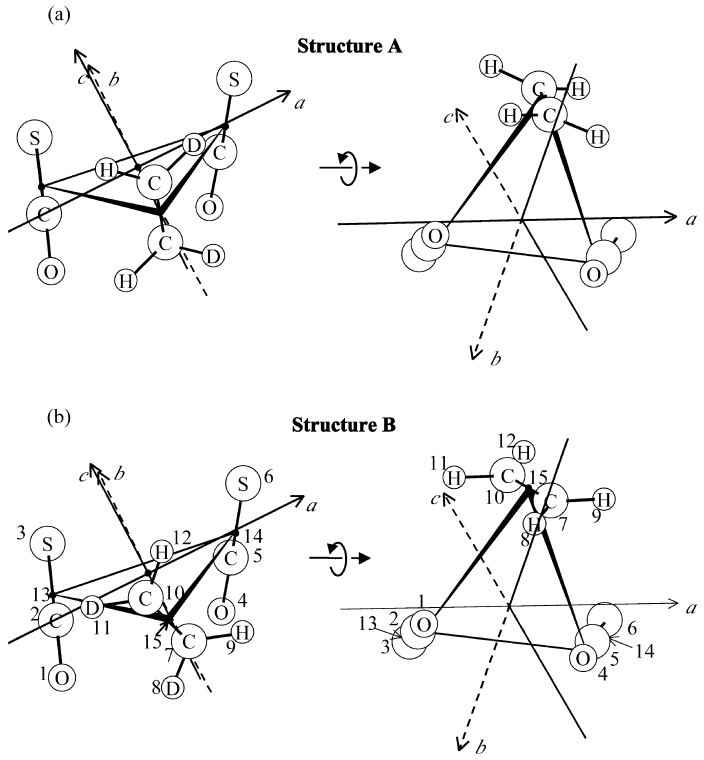

Fig. 1. Two possible structures for C_2H_4–$(OCS)_2$ showing atom numbering scheme and location of deuterium substitution for each structure. Structure A is favored.

mesh plates measuring about 50 cm × 50 cm which were placed just outside the Fabry–Perot cavity of the spectrometer. The plate separation was about 30 cm and the electric field was aligned perpendicular to the microwave propagation axis, giving rise to $\Delta M = 0$ transitions. Calibration of the electric field was achieved by measurement of the Stark effect of the $1 \leftarrow 0$ transition of OCS, assuming a dipole moment of 0.71521 D [20].

The rotational spectra of the isotopic species were measured with commercially available isotopically enriched samples. Spectra for the following isotopomers were observed: C_2H_4–$(O^{13}CS)_2$, C_2H_4–$O^{13}CS$–$O^{12}CS$, C_2H_4–$O^{12}CS$–$O^{13}CS$, $^{13}C_2H_4$–$(OCS)_2$, CH_2CD_2–$(OCS)_2$ and *cis*-CHDCHD–$(OCS)_2$. The second and third isotopomers were observed by mixing equal parts of normal OCS and $O^{13}CS$ with ethylene. The $O^{13}CS$ (99% ^{13}C) was purchased from Isotec; $^{13}C_2H_4$ (99% ^{13}C) was manufactured by Cambridge Isotope Labs; *cis*-CHDCHD (99% D) was manufactured by MSD Isotopes, and the other deuterated species (CH_2CD_2, 99.7% D) was purchased from CDN Isotopes.

3. Results

3.1. Spectra

The 39 observed transitions for the normal isotopomer were fit to a Watson A-reduction Hamiltonian in the I^r representation. Each transition was split into a tunneling doublet by 30–100 kHz. This doubling of rotational transitions is ascribed to an internal motion of the ethylene unit in the trimer from deuterium isotopic data discussed later and by analogy to the ethylene–OCS dimer [16]. Because of the smallness of the splittings, no effort was made to estimate a barrier. All three selection rules were observed, although the *c*-type transitions were strongest corresponding to the largest dipole moment component. The average transition frequencies of the doublets

Table 4
Stark coefficients for the complete dipole moment fit for C_2H_4–$(OCS)_2$

Transition	$\|M\|$	$\Delta\nu/E^{2a}$	Observed−calculated[a]
3_{12}–2_{02}	1	0.5820	0.0576
	2	2.0501	−0.0273
3_{22}–2_{12}	0	0.0232	0.0051
	1	−0.5908	−0.0646
	2	−2.1539	0.0050
3_{21}–2_{11}	1	0.1237	0.0008
	2	0.5360	−0.0174
3_{31}–2_{21}	0	0.0039	−0.0011
4_{13}–3_{12}	0	−0.0073	−0.0010
	1	−0.0112	−0.0010
	2	−0.0239	−0.0023
	3	−0.0455	−0.0050
4_{22}–3_{12}	0	−0.0093	−0.0018
	1	0.0450	0.0076
	2	0.1954	0.0236
	3	0.4163	0.0204

[a] Units of 10^{-4} MHz cm^2 V^{-2}. Calculated values obtained with the dipole components labeled 'complete' in Table 5.

and residuals of the fit for the seven isotopic species are listed in Tables 1 and 2. The spectroscopic constants are given in Table 3. Only one of the two possible species was observed for each of the deuterium isotopomers. This is presumably due to an isotope effect, which causes the second species to be too weak to observe due to jet cooling and conformer relaxation. For the 1,1-d_2 species the identity of the observed spectrum is clear; the CD_2 end is closer to the O···O end of the OCS pair (Fig. 1). For the 1,2-d_2 species, the orientation is ambiguous. Because of this, two structure fits were performed, assigning the observed 1,2-d_2 spectrum to each of the possible configurations as shown in Fig. 1. The absence of splitting in both deuterated spectra is consistent with rotation of the ethylene in its molecular plane. This motion causes an interchange of equivalent hydrogen atoms in the normal species. In the partially deuterated species, hydrogen is replaced by deuterium by this internal rotation leading to two distinct species and the absence of tunneling doublets. This symmetry effect seems more likely to be the origin of the doublet quenching although a simple mass effect reduction cannot be completely precluded, nor a readjustment of the structure to another isomeric form (see later).

3.2. Dipole moment

The Stark shifts for sixteen M components from six transitions were measured. A standard least-squares procedure using calculated Stark coefficients from second order perturbation theory was used to determine the dipole moment of the complex. A fit of all 16 lobes led to dipole moment components of $\mu_a = 0.617(25)$ D, $\mu_b = 0.382(55)$ D and $\mu_c = 0.854(9)$ D with $\mu_{\text{total}} = 1.121(24)$ D. The magnitude of these components is consistent with a parallel dipole alignment for the two OCS moieties. This aspect of the structure will be addressed further in Section 4.

Two other fits of the Stark effect data were examined. One included only components that shift quickly with increased field (Stark coefficient of 10^{-3} or 10^{-4} MHz cm^2 V^{-2}), while the other included only slow moving components (Stark coefficient of 10^{-5} or 10^{-6} MHz cm^2 V^{-2}). Table 4 gives the summary of all Stark coefficients. The 'fast' fit included eight components and led to dipole moment values of $\mu_a = 0.615(45)$ D, $\mu_b = 0.37(10)$ D, $\mu_c = 0.855(16)$ D and $\mu_{\text{total}} = 1.118(44)$ D. These values compare well with the values from the complete fit, although the uncertainties are larger. The 'slow' fit, however, gives different results. They are $\mu_a = 0.649(10)$ D, $\mu_b = 0.423(7)$ D, $\mu_c = 0.942(6)$ D and $\mu_{\text{total}} = 1.219(7)$ D. This fit used only seven components, yet it has much lower uncertainties than the fast and complete fits. Inhomogeneities in the applied electric field which vary with the strength of the field are the likely origin of this variation in the derived dipole moments. Results from the three dipole fits are summarized in Table 5. Based on the variation in the results, the following are recommended values for the dipole moment components: $\mu_a = 0.63(5)$ D, $\mu_b = 0.40(5)$ D, $\mu_c = 0.90(10)$ D and $\mu_{\text{total}} = 1.20(10)$ D.

3.3. Structure

Ten parameters are required to define the structure of the C_2H_4–$(OCS)_2$ trimer. They were determined by least-squares fits to the moments of inertia of the seven isotopomers including the normal species. The atom numbering scheme and parameters chosen are shown in Fig. 1 and Table 6 [21]. It was assumed that monomer structures remained unchanged from their

Table 5
Dipole moment components for $(OCS)_2$–C_2H_4

	Complete[a]	Slow[a]	Fast[a]	Expt. proj. structure A[b]	Expt. proj. structure B[b]	ORIENT structure 2[c]	Induction structure 2[d]	ORIENT structure 4[c]	Induction structure 4[d]
μ_a (D)	0.617(25)	0.649(10)	0.615(45)	0.665	0.661	0.823	0.696	0.892	0.754
μ_b (D)	0.382(55)	0.423(7)	0.38(10)	0.678	0.677	0.623	0.440	0.300	0.068
μ_c (D)	0.854(9)	0.942(6)	0.855(16)	1.001	1.013	1.011	0.917	1.130	1.072
μ_{total} (D)	1.121(24)	1.219(7)	1.118(44)	1.380	1.386	1.188	1.232	1.471	1.312

[a] See text for a description of the different dipole moment fits. The preferred values are, respectively, 0.63(5), 0.40(5), 0.90(10) and 1.20(10) D.
[b] Projections of the monomer moments onto the principal axes of structure A or B.
[c] Obtained using the semi-empirical model (ORIENT) described in text, not including induction effects.
[d] Obtained through a distributed polarizability calculation using ORIENT as described in the text, includes induction effects.

Table 6
Fit parameters for structures A and B and two structures from ORIENT. Distances, R are in Å, and angles, θ and ϕ are in degrees

	Structure A	Structure B	ORIENT structure 2[a]	ORIENT structure 4[a]
R (cm_{13}–cm_{14})	3.852(9)	3.849(9)	3.747	3.761
R (cm_{14}–cm_{15})	3.648(15)	3.673(14)	3.473	4.114
θ (cm_{13}–cm_{14}–cm_{15})	60.53(50)	60.06(47)	58.86	50.66
θ (S_6–cm_{14}–cm_{13})	117.7(16)	117.4(17)	122.44	121.60
θ (S_3–cm_{13}–cm_{15})	108.0(27)	107.3(29)	104.99	107.30
θ (C_{10}–cm_{15}–cm_{14})	87.3(17)	103.6(18)	88.04	139.37
ϕ (S_6–cm_{14}–cm_{13}–cm_{15})[b]	−93.0(36)	−94.0(37)	−87.49	−91.52
ϕ (S_3–cm_{13}–cm_{15}–cm_{14})	−62.6(23)	−62.3(24)	−59.55	−62.68
ϕ (C_{10}–cm_{15}–cm_{14}–cm_{13})	−97.0(27)	−69.9(28)	−82.96	−40.10
ϕ (H_{11}–C_{10}–cm_{15}–cm_{14})	130.0(10)	110.9(15)	119.44	112.95
S.d.[c]	0.168	0.167	–	–

[a] Calculated using the default pre-exponential factor of $K = 0.001E_h$.
[b] Signs of the dihedral angles are consistent with the definition in Ref. [21].
[c] Standard deviation in the fitted moments of inertia, units of amu Å^2.

uncomplexed values (OCS: $r_{OC} = 1.1561$ Å, $r_{CS} = 1.5651$ Å; C_2H_4: $r_{CH} = 1.085$ Å, $r_{CC} = 1.339$ Å, $\theta_{HCC} = 121.1°$) [22]. The configuration of the *cis*-CHDCHD isotopomer in the complex was ambiguous. Structural data obtained without the use of this isotopomer indicate that there should be two distinct 1,2-d_2 species, but only one of these species was observed. The similarity of the predicted rotational constants for the two species, however, makes it impossible to determine which spectrum was assigned. Thus, fits were performed for each of the possible assignments. The results were comparable in quality, but differed structurally.

The two structures obtained align the two OCS units roughly parallel to each other with their dipole moments also aligned parallel. The ethylene is in a plane above the plane of the OCS molecules. The C=C axis is twisted relative to the OCS axes in

Table 7
Principal axis coordinates (in Å) for $(OCS)_2$–C_2H_4. Numbers in absolute value signs are Kraitchman substitution coordinates for C_2 and C_5

	a		*b*		*c*	
	Structure A	Structure B	Structure A	Structure B	Structure A	Structure B
O_1	−2.4781	−2.4816	−0.4533	−0.4194	−0.9741	−1.0244
C_2	−2.0875	−2.0800	0.3494	0.3692	−0.2395	−0.2804
	|2.055|		|0.359|		|0.262|	
S_3	−1.5588	−1.5362	1.4361	1.4367	0.7550	0.7266
O_4	0.8998	0.9433	0.0166	−0.0137	−1.7124	−1.6918
C_5	1.5850	1.6100	0.3098	0.2921	−0.8286	−0.7982
	|1.581|		|0.379|		|0.787|	
S_6	2.5126	2.5126	0.7067	0.7060	0.3679	0.4116
C_7	−0.1562	0.1544	−2.6406	−2.6428	0.0868	0.0921
H_8	−1.1932	−0.5679	−2.8495	−2.7053	−0.1543	−0.7151
H_9	0.5725	1.1929	−2.7057	−2.8531	−0.7143	−0.1408
C_{10}	0.2120	−0.2236	−2.3133	−2.3170	1.3319	1.3347
H_{11}	−0.5168	−1.2622	−2.2482	−2.1067	2.1330	1.5675
H_{12}	1.2489	0.4986	−2.1044	−2.2545	1.5731	2.1419
cm_{13}	−1.9098	−1.8972	0.7147	0.7280	0.0948	0.0581
cm_{14}	1.8968	1.9134	0.4432	0.4312	−0.4264	−0.3915
cm_{15}	0.0279	−0.0346	−2.4770	−2.4799	0.7094	0.7134

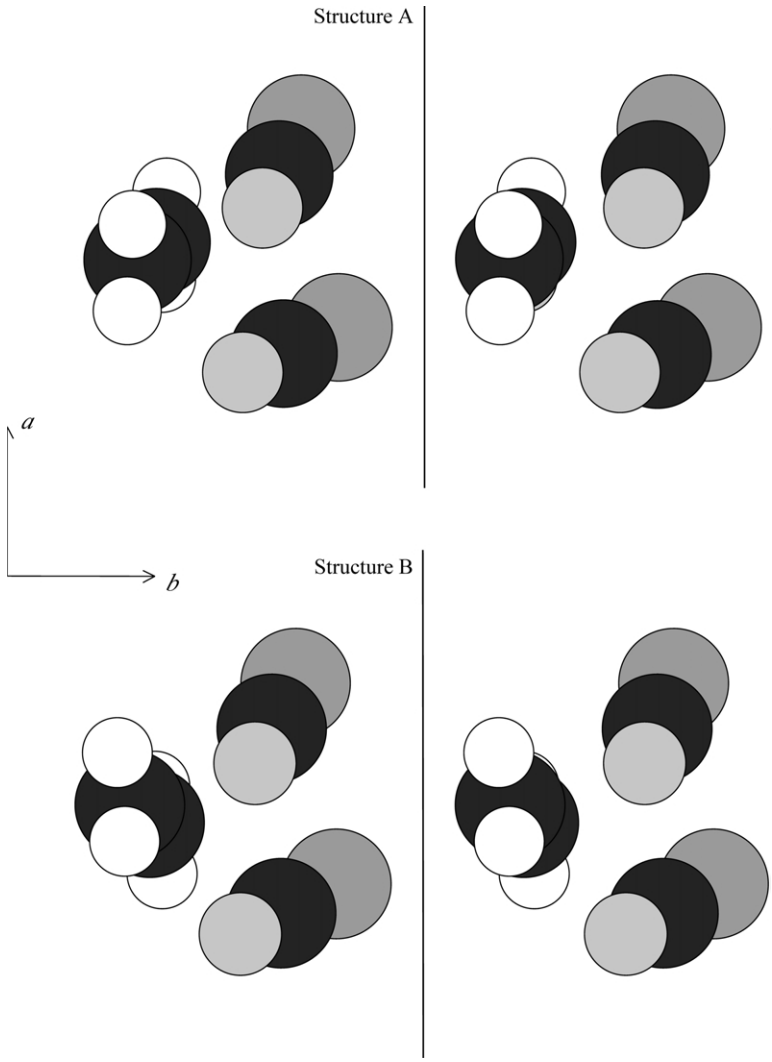

Fig. 2. Stereo images of structures A and B with *ab* plane parallel to the page.

structure B (Fig. 1(b)), while in structure A (Fig. 1(a)) it is roughly parallel to the OCS axes. The assignment of the *cis*-1,2-d_2 species for the two fits is also indicated in the figure. Structural parameters and standard deviations for the two configurations are given in Table 6, and their principal axis Cartesian coordinates are given in Table 7. From the Cartesian coordinates of the ethylene moiety, one can see that the two inertial fits of similar quality arise because the signs of the atom coordinates are ambiguous due to their quadratic dependence on the inertial moments.

Assignment of the two C_2H_4–$O^{13}CS$–$O^{12}CS$ species allowed the determination of Kraitchman substitution coordinates for the two OCS carbon atoms [23]. These values and coordinates from the least-squares structure fitting procedure are given in Table 7. It can be seen that the agreement is excellent, with most differences for both structures under 0.04 Å. The only larger differences are for the relatively small *b*-coordinate of C_5, where structure B differs from the substitution structure by about 0.1 Å. This large difference is easily rationalized for such a small coordinate, since squares of distances are determined in the substitution procedure, and

Table 8
Rotational constants, energies and dipole moment components for various C_2H_4–$(OCS)_2$ structures predicted by the ORIENT semi-empirical model (the experimental rotational constants are 1318.2, 841.8 and 684.4 MHz)

	Structure 1	Structure 2		Structure 3	Structure 4	
	1a	2a	2b	3a	4a	4b
$K(E_h$[a]$)$	0.0010	0.0010	0.0012	0.0010	0.0010	0.0012
Energy (kJ)	−20.1	−19.3	−16.8	−18.5	−18.1	−15.7
A (MHz)	1297.6	1467.4	1412.5	1329.3	1468.5	1403.2
B (MHz)	946.0	873.2	837.2	881.1	811.1	784.2
C (MHz)	848.5	728.7	694.7	786.5	684.3	653.2
μ_a (D)	0	0.82	0.80	0.15	0.89	0.87
μ_b (D)	0.48	0.62	0.61	0.38	0.30	0.31
μ_c (D)	0	1.01	1.04	0.01	1.13	1.14
μ_{total} (D)	0.48	1.44	1.44	0.41	1.47	1.47

[a] Value of K assumed in Eq. (1).

uncertainties become magnified for values close to zero. There is no clear preference for one structure over the other based on comparison with the substitution coordinates or the standard deviation of the fits, since agreement for both configurations is excellent. It should also be noted that the parameters obtained through the least-squares fitting procedure are average values (so called effective or r_0 values) over the large motions that the monomer units undergo in the ground state. The equilibrium structure is probably within ±0.05 Å and 5° of the reported values.

4. Discussion

The centers of mass of the monomers in the C_2H_4–$(OCS)_2$ trimer form an approximately equilateral triangle with the OCS and C=C axes roughly perpendicular to this plane. The two OCS monomers have their dipoles aligned parallel to each other and the plane of the ethylene molecule is sitting above the nearly planar OCS–OCS dimer. Compelling evidence for the polar OCS dimer unit in the complex is obtained from the dipole moment data for the trimer. A structure with anti-parallel OCS monomers should have a small dipole moment, since the dipoles of the individual molecules should largely cancel. The measured dipole moment for the complex, however, is about 1.1 D. This agrees quite well with the assumption that the total moment should be about twice the OCS dipole, or 1.4 D, for a parallel dipole alignment. The similarity of the parameters and the quality of the fits for the two 'parallel' structures makes it impossible to distinguish which is correct, but a semi-empirical model argument presented presently will slightly favor structure A. Fig. 2 shows stereo images of the two structures.

The structure of the C_2H_4–$(OCS)_2$ trimer was modeled using the ORIENT semi-empirical program [17]. This model uses ab initio distributed multipole moments (DMM's), calculated with the CADPAC suite of programs [24], to represent the electrostatic charge distribution in each monomer. Dispersion and repulsion terms are calculated using an exp-6 potential of the form:

$$U_{\exp-6} = \sum_{i,j} K \exp[-\alpha_{ij}(R_{ij} - \rho_{ij})] - \frac{C_6^{ij}}{R_{ij}^6}. \quad (1)$$

In this expression, α, ρ and C_6 are atom–atom terms from Mirsky [25] that are tabulated in Table 11.2 of Ref. [26]. K is a pre-exponential factor which can be adjusted to give better distance agreement between the model and experiment. For this work the default value of $0.001E_h$ for K was used, and a value of $0.0012E_h$, which reproduces experimental distances relatively well was also employed. The DMM's were calculated at the SCF level using a TZ2P basis set from the CADPAC library [24] (see Ref. [16] and references therein for tabulations of the DMM's). Induction effects were not included in the minimization calculations, except to predict their effect on the

dipole moment of the minimum energy structures. This was done by calculating distributed polarizabilities at each atom in the monomers using the CADPAC program and then using an iterative procedure to induce dipoles on each monomer until a constant value was reached. It has been observed in our previous studies that the inclusion of induction effects rarely leads to significant changes in the structure predictions for trimers.

Four structural minima for the C_2H_4–$(OCS)_2$ complex resulted from the ORIENT calculations using $K = 0.001E_h$. Their rotational constants and dipole moments are listed in Table 8. Two of these (structures 2 and 4) had a parallel dipole OCS dimer fragment while the other two (1 and 3) had an anti-parallel dipole OCS dimer alignment. Within each of these pairs one structure had the ethylene C=C axis aligned roughly parallel to the OCS axes, and one had the C=C axis crossed relative to the OCS axes. In all structures, the ethylene plane was roughly parallel to the plane of the OCS molecules. The second and fourth structures roughly resemble the experimental structures A and B, respectively (Fig. 1), although the C=C axis is much more crossed to the OCS axes in structure 4 (see $\phi(C_{10}–cm_{15}–cm_{14}–cm_{13})$ in Table 6). The first and third structures also resemble A and B but with the left-hand OCS rotated by 180° to give nearly anti-parallel dipoles; they can be excluded on this basis. Choosing between structures 2 and 4 is more difficult since the rotational constants of 4 agree slightly better with the experimental values while the lower energy points to 2. Adjustment of the pre-exponential factor K to a value of $0.0012E_h$ which roughly reproduces the experimental center of mass distances makes a choice more obvious. Structure 2 now has distinctly better agreement with the experimental rotational constants as well as the lower energy (Table 8). Additional evidence for structure 2 arises from inclusion of induction in the ORIENT model (with default value of K), which reduces μ_a and μ_b closer to the observed values (Table 5). Structure 2 more closely corresponds to the experimental structure A since the C=C axis is roughly parallel to the OCS axes. The lower energy and better agreement with the rotational constants and dipole components lead us to prefer these structures (ORIENT 2, experimental A) with the more parallel alignment of the C=C and OCS axes.

It should be noted that the small energy differences between the four ORIENT structures suggest that another isomeric form (or several) may exist; therefore, the isomer observed in this study may not be the lowest energy form. An isomer with a non-polar OCS dimer fragment would have a much weaker spectrum due to a smaller dipole moment and could have gone unnoticed to date. The similarity of structures 2 and 4 and their small energy difference indicate that tunneling between these two forms might also be considered as the origin of the tunneling splittings rather than a 180° internal rotation of the ethylene. At this point there is simply not enough information to speculate further on these possibilities except that internal rotation of ethylene about its c-axis in complexes is common, leading to our preference for this dynamical process.

Comparison of the favored ORIENT structure (structure 2) with both fitted configurations elucidates some interesting differences. Table 6 compares the structural parameters for the two experimental configurations and for ORIENT structure 2 as well as 4. It can be seen that most parameters for the two experimental fits are equivalent within the experimental error, but a difference appears for the angle $\theta(C_{10}–cm_{15}–cm_{14})$ and the dihedrals $\phi(C_{10}–cm_{15}–cm_{14}–cm_{13})$ and $\phi(H_{11}–C_{10}–cm_{15}–cm_{14})$. These angles define the orientation of the C_2H_4 moiety with respect to the OCS molecules. The larger θ and smaller dihedral angles for structure B indicate that the ethylene is more crossed relative to the OCS molecules in this configuration, while in structure A the ethylene axis is roughly parallel to the OCS axes. Although the ORIENT prediction of the dihedral angles (structure 2) is intermediate between structures A and B, the angle $C_{10}–cm_{15}–cm_{14}$ is clearly in better agreement with structure A; since A is the favored structure, comparison will be made with it subsequently. The difference between the second dihedral angle and the ORIENT predictions can be attributed to the uncertainty in determining the angle experimentally. Comparison of the ORIENT configuration with experiment shows that distances are within 0.2 Å, and angles are within about 5°, but two of the dihedral angles (including the one mentioned earlier) differ from the experimental structure by 10–15°. These angles are less well determined due to lack of isotopic data for C_2H_4, so this is not surprising. It is apparent

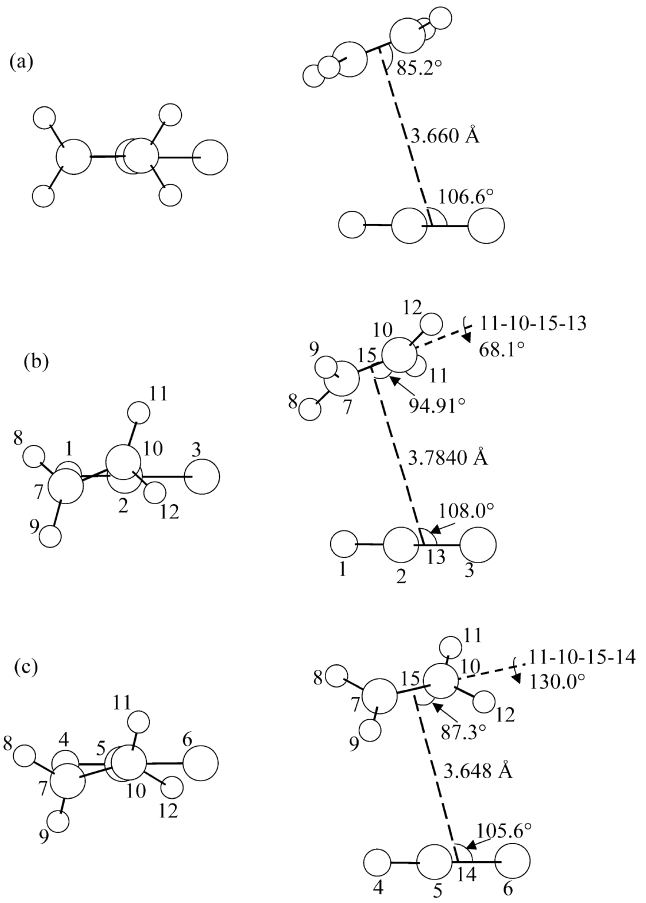

Fig. 3. (a) Ethylene–OCS dimer. (b), (c) Ethylene–OCS faces of C_2H_4–$(OCS)_2$ (structure A).

that the semi-empirical structure is close enough to the experimental values to be a very useful tool for assigning and predicting spectra, although the agreement is far from ideal in the details. In particular, the exact twist of the ethylene moiety above the OCS dimer unit is relatively uncertain. This makes little difference in the predicted rotational constants and dipole moment but it is a significant structural point. Improving the agreement between the experimentally derived structures and the ORIENT predictions requires further work, which is beyond the scope of this study.

It is appropriate to compare C_2H_4–$(OCS)_2$ with C_2H_4–OCS and $(OCS)_2$. The C_2H_4–OCS dimer has recently been studied, and it has a stacked structure with the monomer axes aligned parallel to each other [16]. The two tunneling motions that were observed were attributed to rotation of the ethylene in its molecular plane and rotation of the ethylene around the C=C axis. Fig. 3 shows the isolated dimer and the two C_2H_4–OCS faces of C_2H_4–$(OCS)_2$. The first comparison is between center of mass distances in the two trimer faces and the isolated dimer. The dimer distance is 3.660 Å. This is about 0.12 Å smaller than the distance on face 1 of the trimer but nearly the same as on face 2. This contrast appears to be common to many trimeric systems. It is an indication of the competition between maintaining the clearly favorable interactions that are present in the dimer while adding a third body to the system in an energetically favorable orientation. Comparison of the angles that orient the ethylene and OCS relative to each other shows similar changes. The $C_{ethylene}$–cm–cm angle in the dimer is 85.2°. Again, this shows

Table 9
Comparison of parameters governing the polar OCS dimer portions of various trimers

	C_2H_4–$(OCS)_2$	HCCH–$(OCS)_2$	$(OCS)_3$
R_{cm}(Å)	3.852	3.872	3.843
$\theta(S_3–cm–cm)$ (°)	78.5	83.1	84.8
$\theta(S_6–cm–cm)$ (°)	117.7	117.8	117.9
ϕ(S–cm–cm–S) (°)	27.5	36.1	30.8

excellent agreement with face 2 of the trimer (2.1° difference) but poorer correspondence with face 1 (nearly 10° different). The S–cm–cm angle of the isolated dimer is 106.6°. This value is within 2° of both trimer faces. Perhaps this indicates stronger interactions involving the sulfur atom, and thus less tendency to deviate from the dimer structure.

The S–cm–cm–C dihedral angles are the last parameter to compare. In the dimer, this angle is 0° due to the plane of symmetry which is present, but this symmetry is broken in the trimer. Face 1 has an angle of 68.1° while face 2 has an angle of 130.0°. The difference between these angles reflects the major part of the distortion of the dimer upon adding a third body to the system. While dimeric systems usually have a high level of symmetry, it is impossible to maintain this symmetry in trimers. The monomer units are able to twist and turn to improve the intermolecular interactions in the trimer. While the interactions frequently maintain intermolecular planar angles close to dimer values, at least on one face, dihedral angles are more drastically modified.

The parallel form of OCS dimer has not been detected in the microwave spectral region, although evidence of its existence has been observed [27]. Several recently assigned trimers contain the parallel $(OCS)_2$ unit, however, and a comparison of these faces of the trimers will be made here. The parameters of the $(OCS)_2$ faces from various trimers are summarized in Table 9 and Fig. 4. It can be seen that all three structures are quite similar. This similarity may be a good indication of what the structure of the isolated complex is likely to be. The slight variation in configurations leads to a useful range of structural predictions for the dimer. Ongoing attempts are being made to identify this higher energy form of $(OCS)_2$.

The non-OCS dimer portions of C_2H_4–$(OCS)_2$ also resemble the equivalent HCCH complex quite well. In this trimer, the acetylene unit was slightly twisted

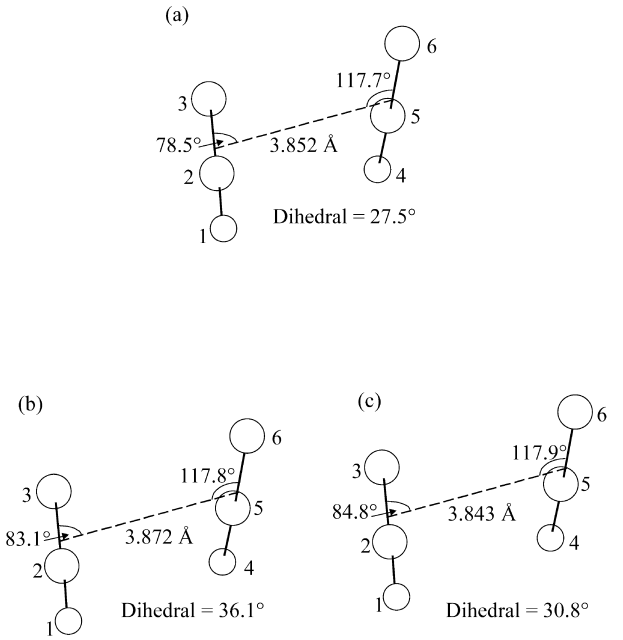

Fig. 4. Polar OCS dimer faces of various trimers. (a) C_2H_4–$(OCS)_2$ (structure A). (b) C_2H_2–$(OCS)_2$. (c) $(OCS)_3$.

relative to the OCS axes as was observed for C_2H_4–$(OCS)_2$. A comparison of the angle and dihedral angle orienting the acetylene or ethylene relative to the OCS molecules shows that the C–cm–cm angle in HCCH–$(OCS)_2$ (103.7°) is 0.1° different from structure B and about 16° different from structure A in the ethylene complex, while the C–cm–cm–cm dihedral (−63.4° in the acetylene complex) differs by about 6° from structure B and by about 34° from structure A. Clearly, comparison with $(OCS)_2$–C_2H_2 favors structure B, in contrast to the semi-empirical evidence. The cm_{OCS}–$cm_{acetylene}$ distances in the acetylene complex are slightly shorter than in the ethylene complex (3.682 and 3.531 Å vs. 3.784 and 3.648 Å for structure A). This difference can be accounted for by the larger overall van der Waals radius of ethylene (due to the hydrogen atoms). A similar, albeit much smaller, trend can be observed in comparing C_2H_4–OCS and C_2H_2–OCS dimers where the distance in the acetylene complex is about 0.05 Å shorter than in the ethylene complex. It appears from the similarity of the structures of the two trimers that the intermolecular interactions in both complexes must be very similar.

5. Summary

The structure of the C_2H_4–$(OCS)_2$ trimer has been determined, and its dipole moment has been measured. A parallel, polar OCS dimer unit has been identified unambiguously through structural and dipole moment analysis, lending further credence to the possibility of this species existing as an isolated dimer. The structure is similar to previously studied trimers containing only linear monomers, and especially resembles the HCCH–$(OCS)_2$ complex. The trimer also compares fairly well with the OCS–C_2H_4 dimer, although only one tunneling motion was observed (due to rotation of ethylene in its molecular plane) compared to two in the dimer. The structure of one trimer face resembles the dimer more closely than the second face. This is a trend which has been observed in the majority of the trimers involving linear monomers which have been studied. This retention (in part) and distortion of the dimer configuration apparently represents the best trade-off between maintaining favorable dimer interactions while introducing additional interactions that arise upon addition of a third monomer moiety to the system.

Acknowledgements

The spectrometers used in this study were constructed and maintained by grants from the Experimental Physical Chemistry Program, National Science Foundation, Washington DC. RAP acknowledges support from a Margaret Sokol Fellowship from the University of Michigan Department of Chemistry.

The Michigan microwave spectroscopists warmly recall many interactions and collegial support from the Kiel spectroscopy group over the years.

References

[1] T.J. Balle, W.H. Flygare, Rev. Sci. Instrum. 52 (1981) 33.
[2] S.A. Peebles, R.L. Kuczkowski, Chem. Phys. Lett. 286 (1998) 421.
[3] S.A. Peebles, R.L. Kuczkowski, J. Chem. Phys. 109 (1998) 5276.
[4] S.A. Peebles, R.L. Kuczkowski, J. Phys. Chem. 102 (1998) 8091.
[5] R.A. Peebles, S.A. Peebles, R.L. Kuczkowski, Mol. Phys. 96 (1999) 1355.
[6] S.A. Peebles, R.L. Kuczkowski, J. Mol. Struct. Theochem 500 (2000) 391.
[7] S.A. Peebles, R.L. Kuczkowski, J. Chem. Phys. 111 (1999) 10511.
[8] M.J. Weida, D.J. Nesbitt, J. Chem. Phys. 10210 (1996) 105.
[9] J.P. Connelly, A. Bauder, A. Chisholm, B.J. Howard, Mol. Phys. 915 (1996) 88.
[10] G.T. Fraser, A.S. Pine, W.J. Lafferty, R.E. Miller, J. Chem. Phys. 1502 (1987) 87.
[11] H.S. Gutowsky, J. Chen, P.J. Hajduk, R.S. Ruoff, J. Phys. Chem. 7744 (1990) 94.
[12] R.E. Miller, L. Pedersen, J. Chem. Phys. 436 (1998) 108.
[13] R.S. Ruoff, T. Emilsson, T.D. Klots, C. Chuang, H.S. Gutowsky, J. Chem. Phys. 138 (1998) 89.
[14] K.W. Jucks, R.E. Miller, J. Chem. Phys. 2196 (1988) 88.
[15] R.A. Peebles, S.A. Peebles, R.L. Kuczkowski, J. Chem. Phys. 112 (2000) 8839.
[16] S.A. Peebles, R.L. Kuczkowski, Mol. Phys. 99 (2001) 225.
[17] A.J. Stone, A. Dullweber, M.P. Hodges, P.L.A. Popelier, D.J. Wales, ORIENT: A Program for Studying Interactions Between Molecules, University of Cambridge, Cambridge, 1995 Version 3.2.
[18] K.W. Hillig II, J. Matos, A. Scioly, R.L. Kuczkowski, Chem. Phys. Lett. 133 (1987) 359.
[19] J.-U. Grabow, PhD thesis, University of Kiel, Kiel, 1992.
[20] J.S. Muenter, J. Chem. Phys. 48 (1968) 4544.

[21] E.B. Wilson, J.C. Decius, P.C. Cross, Molecular Vibrations, McGraw-Hill, New York, 1955.
[22] M.D. Harmony, V.W. Laurie, R.L. Kuczkowski, R.H. Schwendeman, D.A. Ramsay, F.J. Lovas, W.J. Lafferty, A.G. Maki, J. Phys. Chem. Ref. Data 8 (1979) 619.
[23] J. Kraitchman, Am. J. Phys. 21 (1953) 17.
[24] CADPAC: The Cambridge Analytic Derivatives Package Issue 6, Cambridge, 1995. A suite of quantum chemistry programs developed by R.D. Amos with contributions from I.L. Alberts, J.S. Andrews, S.M. Colwell, N.C. Handy, D.Jayatilaka, P.J. Knowles, R. Kobayashi, K.E. Laidig, G. Laming, A.M. Lee, P.E. Maslen, C.W. Murray, J.E. Rice, E.D. Simandiras, A.J. Stone, M.-D. Su and D.J. Tozer.
[25] K. Mirsky, in: R. Schenk, R. Olthof-Hazenkamp, H. Van Koningveld, G.C. Bassi (Eds.), The Determination of Intermolecular Interaction Energy By Empirical Methods, Delft University Press, Delft, The Netherlands, 1978.
[26] A.J. Stone, The Theory of Intermolecular Forces, Clarendon Press, Oxford, UK, 1996.
[27] J.M. LoBue, J.K. Rice, S.E. Novick, Chem. Phys. Lett. 112 (1984) 376.